Available online at www.sciencedirect.com
ScienceDirect
Biochimica et Biophysica Acta 1774 (2007) 121 – 130
Biochimica et Biophysica Acta
BBA
www.elsevier.com/locate/bbapap

The pH dependence of the activity of dehaloperoxidase from *Amphitrite ornata*

Stefan Franzen *, Lauren B. Gilvey, Jennifer L. Belyea

Department of Chemistry, North Carolina State University, Raleigh, NC 27695, USA

Received 2 August 2006; received in revised form 18 September 2006; accepted 29 September 2006
Available online 1 November 2006

Abstract

Dehaloperoxidase (DHP) from the terebellid polychaete, *Amphitrite ornata,* is the first hemoglobin that has peroxidase activity as part of its native function. The substrate 2,4,6-tribromophenol (TBP) is oxidatively debrominated by DHP to form 2,6-dibromoquinone (DBQ) in a two-electron process. There is a well-defined internal binding site for TBP above the heme, a feature not observed in other hemoglobins or peroxidases. A study of the pH dependence of the activity of DHP reveals a substantial difference in mechanism. From direct observation of the Soret band of the heme it is shown that the pK_a for heme activation in protein DHP is 6.5. Below this pH the heme absorbance decreases in the presence of H_2O_2 with or without addition of substrate. The low pH data are consistent with significant heme degradation. Above pH 6.5 addition of H_2O_2 causes the heme to shift rapidly to a compound II spectrum and then slowly to an unidentified intermediate with an absorbance of 410 nm. However, the pK_a of the substrate TBP is 6.8 and the greatest enzyme activity is observed above the pK_a of TBP under conditions where the substrate is a phenolate anion ($TPBO^-$). Although the mechanisms may differ, the data show that both neutral TBP and anionic $TPBO^-$ are converted to the quinone product. The mechanistic implications of the pH dependence are discussed by comparison other known peroxidases, which oxidize substrates at the heme edge.

Keywords: Peroxidase; Fourier-transform infrared spectroscopy; X-ray crystallography; Enzyme kinetics

1. Introduction

The enzyme dehaloperoxidase (DHP) from the terebellid polychaete *Amphitrite ornata* is a hemoglobin (Hb) with peroxidase activity [1,2]. DHP has recently been expressed in *E. coli* [1]. DHP binds oxygen reversibly and it is highly likely that it possesses a Hb function in *A. ornata*. It is of interest to determine how DHP can switch function from oxygen binding and oxidize halogenated phenols to their corresponding quinones in the presence of H_2O_2. In its habitat in saline mud flats *A. ornata* is exposed to brominated phenols [3]. The native substrate 2,4,6-tribromophenol (TBP) is sparingly soluble below its pK_a of 6.8. In fact, it is only moderately soluble at the pH of the coelom (pH ~7.4). Although previous studies have referred to the substrate as a phenol [1,2,4,5], TBP is largely in its conjugate base form, 2,4,6-tribromophenolate ($TBPO^-$) at the coelomic pH of 7.4. This observation leads to the present investigation of whether there is a difference in activity for the neutral and anionic forms of the substrate.

Substituted phenols are good substrates for a wide range of plant secretory (class III) peroxidases [6–11]. Although chlorophenols are widely studied, most of the work done is at pH < pK_a for the substrate. The optimum activity of most class III peroxidases is at pH < 5.5 and the widely studied substrate 2,4,6-trichlorphenol has pK_a = 6.2. Other halogenated phenols have higher pK_a values. Class III peroxidases oxidize phenols to the corresponding cation in a one-electron oxidation at the heme edge [12]. The loss a proton from the cationic phenol to create the phenoxy radical is an important pH-dependent step for

Abbreviations: CcP, cytochrome *c* peroxidase; DBQ, 2,6 dibromoquinone; DCQ, 2,6 dichloroquinone; DHP, dehaloperoxidase; HRP, horseradish peroxidase; LiP, lignin peroxidase; Mb, myoglobin; P450cam, cytochrome P450 camphor; SVD, singular value decomposition; SWMb, Sperm Whale myoglobin; TBP, 2,4,6 tribromophenol; TCP, 2,4,6 trichlorophenol; 24-DCP, 2,4-dichlorophenol

* Corresponding author. Tel.: +1 919 515 8915; fax: +1 919 515 8920.
E-mail address: Stefan_Franzen@ncsu.edu (S. Franzen).

1570-9639/$ - see front matter © 2006 Published by Elsevier B.V.
doi:10.1016/j.bbapap.2006.09.019

phenolic substrates. In most peroxidases, this step does not appear to be rate limiting since the substrate is at the heme edge in contact with solvent water so that deprotonation is rapid. DHP has a substantially different structure in the distal pocket. DHP has an interior substrate-binding site, which implies that the role of the protonation state of the substrate could be a kinetically limiting step for enzyme function.

The catalytic activity of peroxidases is pH dependent [13–20]. Class I peroxidases, which are usually found inside cells have maximum turnover rates in the range pH 6.0–8.5 depending on whether they are located in the cytosol, periplasmic space or thylakoid [21]. Class I peroxidases include yeast Cytochrome c Peroxidase (CcP), catalase-peroxidases [22] and ascorbate peroxidases [23]. Secreted plant and fungal peroxidases (types II and III) [24–27] tend to have maximum turnover at pH 3.0–5.5. The optimum pH of secretory peroxidases is matched to that of the soil or other environments where the enzymes function. Peroxidase activity in all three classes is limited at high pH (usually pH 9 or greater) by the formation of the ferric hydroxide form (acid-alkaline transition). On the other hand, at low pH (usually pH 4 or less) the protonation of the distal histidine [28] is associated with a change in ligand binding to the heme iron or loss of enzyme activity. In some peroxidases the protonation of the *proximal* histidine limits the activity of peroxidases at low pH [14,29]. Peroxidases that bind calcium ions may also lose activity at low pH due to protonation of aspartates leading to loss of calcium binding [18,26,30,31].

In all known cases, peroxidase activity requires general acid–base catalysis for the activation of hydrogen peroxide to create an active compound I intermediate [32]. This role is played by the distal histidine, H42, in horseradish peroxidase (HRP) [27,33,34] and analogous distal histidines in other peroxidases [17, 35]. A distal arginine and asparagines also play an auxiliary role in proton transfer [13,36–38]. These amino acids catalyze proton transfer from the α-oxygen of H_2O_2 to the β-oxygen leading to heterolytic cleavage of the O − O bond and formation of compound I [38]. DHP lacks these features regarded as essential for activation of bound H_2O_2.

Although DHP has a distal histidine (H55), it lacks the distal arginine that is found in all of the heme peroxidases studied to date. Fig. 1 shows key amino acids from the X-ray crystal structure with a substrate analog, 4-iodophenol, bound in the substrate-binding pocket [4,39]. The substrate-binding pocket is surrounded by hydrophobic residues, including four phenylalanine side chains F21, F24, F35, and F60, as well as residues L25, V59, and Y38 shown in Fig. 1. The hydroxyl group of the substrate may act as a hydrogen bond acceptor for the hydroxyl group of Y38 (Y38-OH...OH-2,4,6-Phenyl). The functional importance of these residues has been shown in a kinetic study of mutations Y38F, H55R, and H55V [1]. There is relatively close contact of 4.9-6.6 Å between the hydroxyl of S56 and the oxygen of 4-iodophenol as well (not shown in Fig. 1). In addition to these residues the only other residue in the distal pocket is H55. H55 is exposed to solvent with the Nε-H > 9 Å from the heme iron in the substrate-bound structure shown in Fig. 1. H55 is also found in two conformations in the DHP

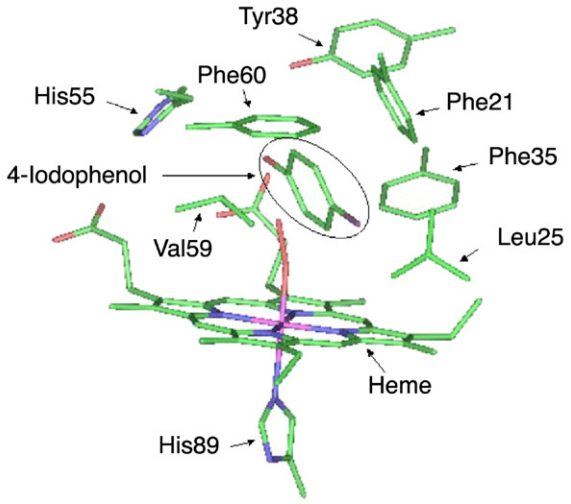

Fig. 1. View of the DHP active based on X-ray crystal structure [PDB #1EW6] that has a substrate analog, 4-iodophenol, bound in a binding site above the heme iron. A model of bound H_2O_2 (without hydrogen atoms) was added to this structure to indicate the close proximity to the substrate.

structure that lack the substrate analog, 4-iodophenol. One histidine conformation is similar to the solvent-exposed configuration shown in Fig. 1 and the other is in an interior conformation that resembles the distal histidine of globins. The conformations of V59 and H55 are remarkably similar to the analogous amino acid residues V68 and H64, but with a 1.5 Å shift relative to the heme [40]. It is likely that the conformation of H55 depends on pH given that the distal histidine of myoglobin (Mb) is known to also have a solvent exposed conformation at pH 4.5 [41]. The protonation of the distal histidine accelerates the autooxidation of Mb [42]. The X-ray crystal structures [4,39], spectroscopic [5] and theoretical [43–45] studies reveal that both distal and proximal geometries of DHP are similar to Mb and quite different in structure from any known peroxidase.

Based on the functional information available from other globins it would appear that DHP is a unique protein in the globin family. To understand whether there is any phylogenetic relationship between members of the Mb family and DHP, a BLAST search was performed for proteins of similar amino acid sequence. In a BLASTP search [46] against the entire database of known sequences using the DHP A amino acid sequence [4,47], there were 6 globin sequences found with a E-values less than 0.01 (see Supporting Information). Of course, this analysis does not include the second DHP gene (DHP B), which obviously has high sequence similarity since it differs by only 5 amino acids from DHP A. Interestingly, the sequence identity is not higher than 26% for any of these proteins with DHP. The two proteins with the highest sequence identity are Mbs from the sea hares (slugs) *Aplysia limacina* [48] ($E = 2 \times 10^{-4}$) and *Aplysia kurodai* [49] ($E = 6 \times 10^{-4}$). The sea hare sequences are also relatively isolated having direct relationship with only a few other sea hares *Bursatella leachii, Dolabella auricularia* and *Aplysia juliana.* The next most closely related group of proteins consists of four Hbs from *Kiefferulus cornishi* [50] ($E = 0.02–0.08$). These hemoglobins have high sequence

homology with a number of other midge globins from the genus *Chironomus*. The proteins with lower sequence homology to DHP A are also Mbs and Hbs. Cytoglobin [51] is the mammalian protein most closely related to DHP. This is relevant since cytoglobin is dimeric and appears to accommodate small molecules in a site above the heme iron [52], and thus bears a structural similarity to DHP. Cytoglobin has also reported to have catalase activity, which is novel in the globin family. Although there is little sequence homology there is structural and perhaps functional similarity between these dimeric hemoglobins.

The investigation of the pH dependence of DHP enzymatic activity is the starting point for an understanding of the novel structure–function relationships in a new class of globins. The present study addresses the charge state of the substrate oxidized by DHP by using pH dependent spectral measurements to determine the kinetics. The data show that the spectral features associated with both the heme and substrate oxidation change dramatically below the pK_a of TBP.

2. Materials and methods

The expression and purification of 6Xhis-DHP from *E. coli* have been discussed in detail elsewhere [1]. In previous studies it has been shown that there is no difference in activity when 6XHis-DHP and native DHP sequences are used [1]. In this study we refer to 6XHis-DHP simply as DHP in figures and legends. Substrate 2,4,6-tribromophenol (TBP) was obtained from Acros Organics. A Hewlett Packard 8453 multi-wavelength spectrometer was used to obtain the relative activities of the mutants. Spectra were obtained every 5 s with a total of 200 spectra per run. Samples were prepared in 100 mM citrate buffer (pH 4.0 and 5.0) or 100 mM potassium phosphate buffer (pH 6.0, 6.5, 7.0 and 8.0). Assay conditions were 6 μM 6XHis-DHP, 650 μM H_2O_2, 600 μM TBP for kinetic assays in Fig. 3 below and 4 μM 6XHis-DHP, 50 μM H_2O_2, and 100 μM TBP in the time-dependent spectra in Figs. 4 and 5.

Spectra were obtained every 5 s with a total of 200 spectra per run. We have found that the use of acetate buffer reported elsewhere [53] can result in heme loss (see Supporting Information). Therefore, only citrate buffer was used to low pH (pH <6) kinetic assays.

Stopped flow measurements were performed on an Applied Photophysics SX.18 MV Stopped-flow Reaction analyzer (Surrey, UK) at constant pressure using excess TBP to maintain pseudo-first-order conditions. For each set of reaction conditions, 25–30 replicates were performed. The progress of the reactions was monitored at 272 nm for the appearance of products and at 316 nm for the decrease in substrate concentration. The results from multiple measurements of each reaction were averaged and fit to an exponential function to determine the rate constant. Constant temperature was obtained by a circulating water bath at 20 °C, and constant pressure was maintained with nitrogen gas. Assay conditions were 6 μM His-DHP, 650 μM H_2O_2, 600 μM TBP, and 10 mM citrate buffer (pH 4.0, 4.5, 5.0 and 5.5) or 10 mM KP buffer (pH 6.0, 7.0, and 8.0) with 0.05 M KNO_3 added.

3. Results

The pH dependence of the kinetics on the time scale of 0 to 10 s is shown in the stopped-flow data in Fig. 2. Fig. 2A shows the rate of appearance of product measured at 272 nm. Fig. 2B shows the rate of consumption of reactants measured at 316 nm. Ordinarily one would expect conditions that lead to greater rate for appearance of product to lead to a larger change in absorbance (ΔA) for the product. This is clearly not the case as shown by the trend obtained from fits to a single exponential function presented in Table 1. The change in ΔA at 272 nm increases from pH 4.0 to pH 7.0, peaks at pH 7.5 and decreases again at pH 8.0. The rate constant is large for low pH (where the amplitude is small), but decreases monotonically above pH 6.0. The rate constant k_{obs} and ΔA are not correlated in the sense that at pH < pK_a the rate constant is large, but less product is formed (i.e. the kinetic traces in Fig. 2A level off after ~3 s), whereas at pH 7.0 the rate constant is much smaller, but it is clear that activity continues for longer than the period of observation by constant pressure stopped-flow (10 s). The fit to the substrate consumption data in Fig. 2B show that the rate constant for is matched to the product formation at pH < 6.0, but ΔA is very small. The reason for this is that the substrate has very little absorbance below pH 6.0 as discussed below. Above pH 6.0 the substrate is consumed as indicated by the large negative change in ΔA, which is largest at pH 7.0 in agreement with the product formation data.

Time-dependent spectra shown in Fig. 3 were obtained using a UV-vis photodiode array spectrometer under the same conditions used for the stopped-flow measurements. These experiments were needed since the stopped-flow instrument can

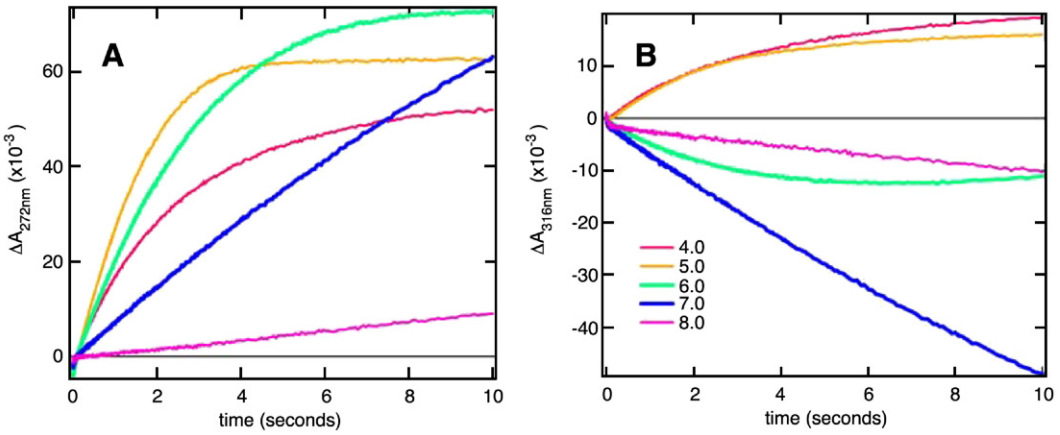

Fig. 2. Single wavelength kinetics of the oxidative debromination of TBP by DHP as a function of pH obtained using stopped-flow measurements. The fits to a single exponential function are presented in Table 1. (A) The kinetics at 272 nm. (B) The kinetics at 316 nm. Assay conditions were 6 μM 6XHis-DHP, 650 μM H_2O_2, and 600 μM TBP.

Table 1
Single exponential fits to the stopped-flow kinetic data as a function of pH

pH	k (s^{-1}) at 272 nm	ΔA (272 nm)	k (s^{-1}) at 316 nm	ΔA (316 nm)
4.0	0.41	0.053	0.34	0.020
4.5	0.49	0.059	0.38	0.020
5.0	0.61	0.068	0.44	0.017
5.5	0.53	0.065	0.032	0.017
6.0	0.36	0.080	0.51	−0.012
7.0	0.060	0.14	0.0612	−0.11
8.0	0.033	0.033	0.225	−0.0096

The assay conditions were 6 μM His-DHP, 650 μM H_2O_2, and 600 μM TBP.

only acquire data for 10 s when used in the required constant-pressure mode. The kinetics are sufficiently slow that there is a large change in absorbance (ΔA) at times longer than 10 s. Fig. 3A shows the time course for product formation and Fig. 3B shows that substrate consumption at 316 nm. Fits to the kinetics corresponding to the data in Fig. 3 show that the overall trends are similar to those observed in the stopped-flow measurements. The most rapid rates are observed at low pH, while by far the largest change in absorbance at a wavelength representative of product formation is observed at pH 7.5. There is little activity at more extreme pH values of 4.0 or 9.0 (data not shown). Given

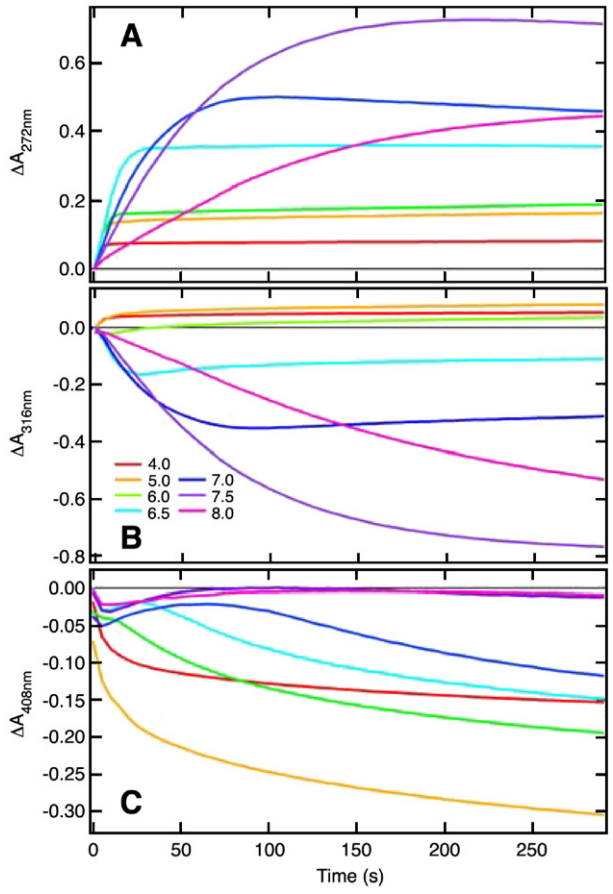

Fig. 3. Single wavelength kinetics of the oxidative debromination of TBP by DHP as a function of pH. The fits to a single exponential function are presented in Table 2. Kinetics are shown at (A) 272 nm. (B) 316 nm and (C) 408 nm. Assay conditions were 6 μM 6XHis-DHP, 650 μM H_2O_2, and 600 μM TBP.

the absence of absorption bands for the substrate at 316 nm there is little signal below pH 6 in Fig. 3B. Fig. 3C shows the change in absorbance of the heme Soret band at 408 nm. At low pH (pH 4 and 5) there is a large decrease in absorbance that is indicative of degradation of the heme. At higher pH the more complicated time course reflects transient formation of compound II as discussed below. The kinetic fits to the product formation at 272 nm and substrate consumption at 316 nm are given Table 2. These data parallel the data from the stopped-flow measurements given in Table 1. Product formation measured at 272 nm is rapid below pH 6.0, it seems to be limited by some other process. Although the kinetics are slower, a much greater yield of product is obtained above pH 6.0 with a maximum at pH 7.5.

During the course of the experiments at pH 6.0 and lower several trials were made in acetate buffer following published procedures [53]. It was observed that there was a scattering background at the wavelength of the product acetate this buffer as shown in the Supporting Information. After some time a green color was observed in samples where acetate buffer was used. As a consequence only citrate buffer was used in the experiments that were analyzed in this study.

In order to assess the significance of the kinetic data, time-dependent spectra were obtained as function of pH. Fig. 4 shows the absorbance of DHP and TBP for pH 5, 6, 7 and 8. Fig. 5 shows the difference spectra corresponding to these absorption spectra. The time span of the experiment is 600 s. The activity is largest at pH 7. This is most evident in the difference spectra in Fig. 5. Note that the spectrum of the substrate, TBP, depends on pH so that the 249 nm and 316 nm bands is not apparent at pH 5 and begins to grow in at pH 6. These observations are consistent with the pK_a of TBP (pK_a=6.8). The changes in the spectrum of TBP as a function of pH are shown more clearly in Fig. 6. Thus, the fact that less change in absorbance at 316 nm is observed at lower pH does not necessarily mean that there is less activity, only that the absorption band for TBP at 316 nm is no longer present.

The heme Soret band can be seen in the spectra. There is a qualitatively different behavior in the Soret band at pH 5 and 6 compared to pH 7 and 8. At low pH the major change in the Soret band spectrum is a loss of intensity with time.

Table 2
Single exponential fits to the UV-vis kinetic data as a function of pH

PH	k (s^{-1}) at 272 nm	ΔA (272 nm)	k (s^{-1}) at 316 nm	ΔA (316 nm)
4.0	0.33	0.12	0.073	0.047
4.5	0.25	0.18	0.084	0.070
5.0	0.18	0.19	0.026	0.059
5.5	0.14	0.15	0.018	0.053
6.0	0.15	0.22	0.0083	−0.054
6.5	0.097	0.43	0.19	−0.18
7.0	0.043	0.55	0.046	−0.39
7.5	0.018	0.79	0.013	−0.84
8.0	0.0086	0.51	0.0043	−0.77

The assay conditions were the same as those used in the stopped-flow kinetic experiments (6 μM His-DHP, 650 μM H_2O_2, and 600 μM TBP).

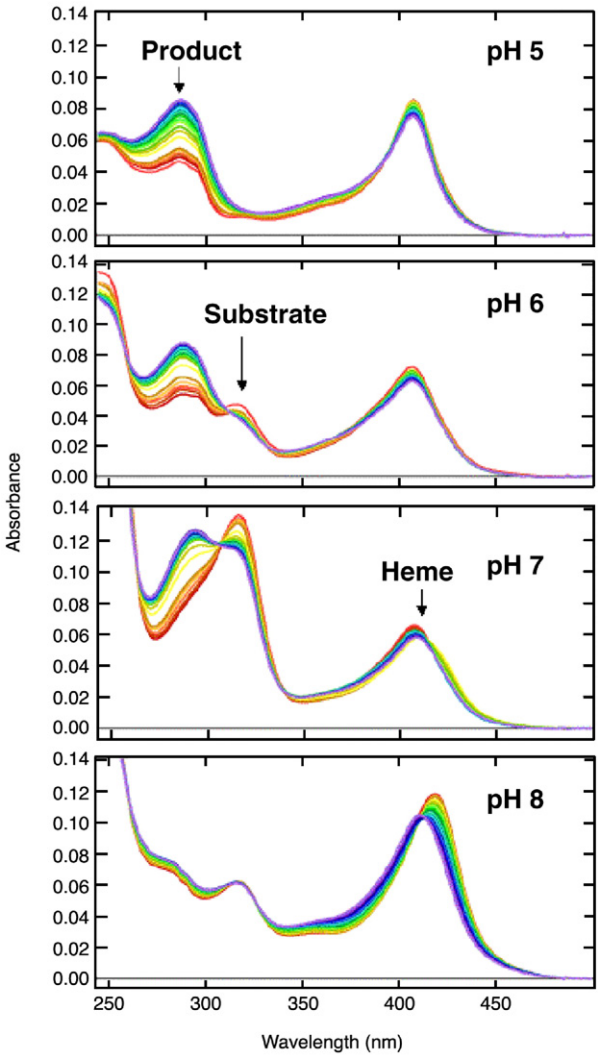

Fig. 4. Time-dependent spectra obtained using the photodiode array spectrometer. The total time course is 600 s (blue) and the earliest time point is 3 s (orange). Assay conditions were 4 μM 6XHis-DHP, 50 μM H_2O_2, and 100 μM TBP.

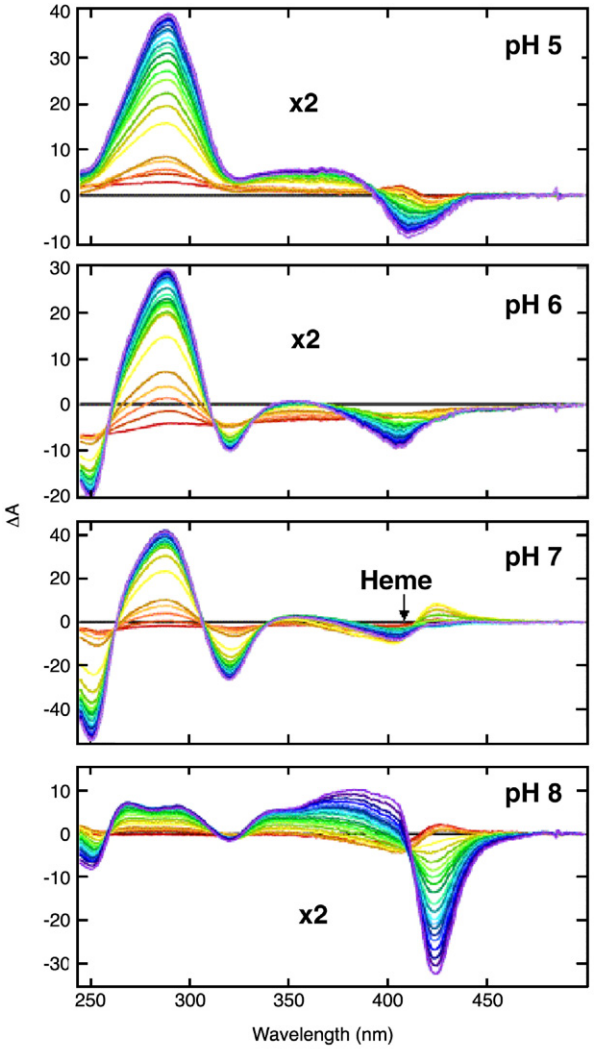

Fig. 5. Time-dependent difference spectra obtained using the photodiode array spectrometer. The total time course is 600 s (blue) and the earliest time point is 3 s (orange). Assay conditions were 4 μM 6XHis-DHP, 50 μM H_2O_2, and 100 μM TBP.

The loss of intensity is only slightly slower than the appearance of product. At pH 7 and 8 there is a shift in the heme absorption band indicative of the formation of compound II. The shift is followed by a relaxation to a wavelength intermediate between the ferric form (407 nm) and the compound II form (419 nm). The spectral shifting of the heme Soret band is even more pronounced at pH 8. At pH 8 it is evident that this shift is not coupled to product formation since there is little activity. The loss of activity at pH 8 is expected because DHP has an unusually low pK_a of 8.1 for the acid–alkaline transition in the ferric form [54,55]. Thus, there is a substantial equilibrium concentration of ferric hydroxide DHP at pH 8.

In order to better understand the origin of the effect on the Soret band itself mixing of DHP and H_2O_2 was performed without substrate at pH 5 and 7, as shown in Figs. 7 and 8, respectively. Fig. 7 shows a loss of Soret band intensity in the presence of H_2O_2 analogous to the change observed when substrate is present. Fig. 8 shows a shift at short time to form

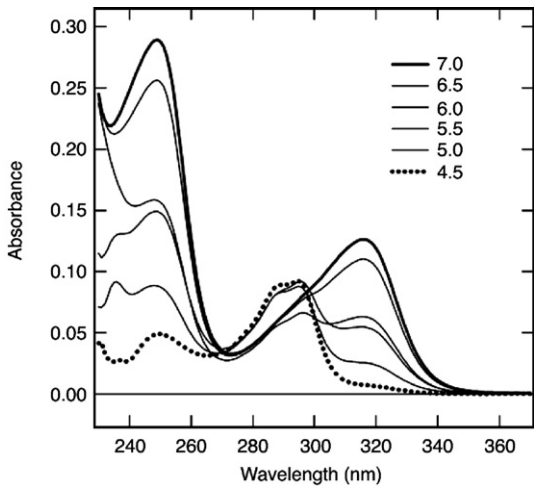

Fig. 6. pH titrations of TBP obtained using a photodiode array spectrometer.

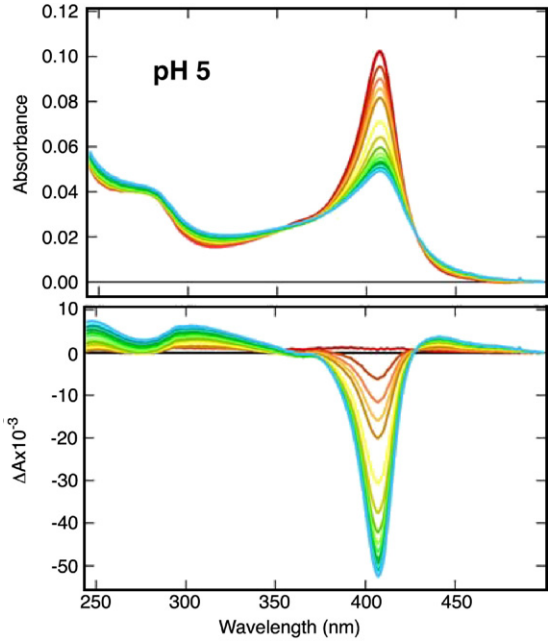

Fig. 7. Time-dependent spectra (top) and difference spectra (bottom) obtained using the photodiode array spectrometer when DHP and H_2O_2 were mixed at pH 5 with no TBP added. The total time course is 600 s (blue) and the earliest time point is 3 s (orange). Assay conditions were 4 μM 6XHis-DHP and 600 μM H_2O_2.

compound II at pH 7.0. The amount of compound II produced is less than when substrate is present. As was observed in the presence of substrate the compound II spectrum relaxes relatively to an intermediate value of 410 nm.

4. Discussion

DHP is found in coelom of *A. ornata* and is likely both a Hb and a peroxidase [56,57]. *A. ornata* also has a high molecular weight vascular Hb [57]. The dimeric structure of DHP [4,39] resembles other dimeric Hbs in marine organisms [58,59]. While early reports indicated that the coelomic Hb of *A. ornata* is monomeric [56], there are also indications that DHP has forms that only have one heme [2]. At high concentration DHP is certainly dimeric, but there are no data on the concentration dependence of dimer formation in DHP. Our hypothesis that DHP is a dual function protein implies that must have adapted to oxidize substrates in ways that differ significantly from the cytochrome *c* peroxidase family of enzymes. In this study we are interested in the consequences of the protonation state of the substrate. Since TBP is the conjugate base form, $TBPO^-$, at the coelomic pH of 7.4 it is of interest to observe the kinetics and spectra of DHP turnover as a function of pH.

There is a change in the spectrum of substrate as it is titrated through its pK_a of 6.8. The absorption spectrum for the phenolate form $TBPO^-$ (pH>6.8) has absorption bands at 316 nm and 249 nm. As a consequence it becomes impossible to monitor the rate of substrate consumption below pH 6.0. Therefore, at pH<6.0 all of our information on the kinetics of turnover must be based on the wavelengths at which the appearance of the product (270–290 nm). Moreover, the substrate acts as an internal pH probe.

The time-dependent spectra reveal that the changes in the heme absorption line shape at low pH (pH 5 and 6) differ from those observed at high pH (pH 7 and 8). This observation suggests that the enzyme mechanism is dependent upon pH. Figs. 7 and 8 suggest that there are some intrinsic differences in the reactivity of the heme towards H_2O_2 as a function of pH. However, it is also possible that the observed differences depend on whether the bound substrate is in a neutral (TBP) or anionic ($TBPO^-$) form.

The results do not follow expected kinetic trends according to which the greater rate constant would be expected to produce the larger yield of product. Under stopped-flow conditions (Figs. 2 and 3) the rate constant for the conversion of substrate to product increase as the pH is lowered. However, the total amount of product decreases as the pH is lowered. One possible explanation is that the enzymatic rate increases as the pH is lowered, but so too does a competing inhibition of the enzyme such as heme degradation by peroxide or a radical intermediate. A second possible explanation for this observation is that the nature of the product distribution is pH dependent. There are two major products that result from peroxidase activation of phenols (or phenolates). The first is a quinone and the second is a polymer formed by a radical pathway.

Following the treatment in many previous studies peroxidases are known to perform either two sequential one-electron oxidations

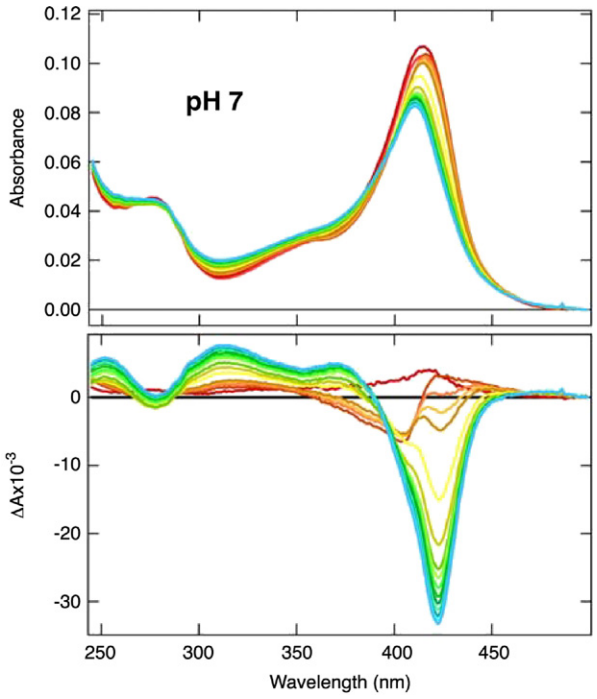

Fig. 8. Time-dependent spectra (top) and difference spectra (bottom) obtained using the photodiode array spectrometer when DHP and H_2O_2 were mixed at pH 7 with no TBP added. The total time course is 600 s (blue) and the earliest time point is 3 s (orange). Assay conditions were 4 μM 6XHis-DHP and 600 μM H_2O_2.

[60] $SH \rightarrow S + H^+ + e^-$ or a single two-electron oxidation [1] $XA–OH + H_2O \rightarrow O{=}A{=}O + HX + 2H^+ + 2e^-$(mechanism A):

$$1A.\ DHP + H_2O_2 \rightarrow \text{Compound I} + H_2O \qquad (k_{1A})$$

$$2A.\ \text{Compound I} + XA–OH \rightarrow \text{N Compound II} + XA–O^{\bullet} + H^+ \qquad (k_{2A})$$

$$3A.\ \text{Compound II} + XA–O^{\bullet} + H^+ \rightarrow DHP + O{=}A{=}O + HX \qquad (k_{3A})$$

where the substrate is XA–OH (XA–OH and O═A═O represent the para-halogen, substituted phenol, and the corresponding quinone, respectively). For substrate TBP the product quinone is 2,6-dibromoquinone, which absorbs between 270 and 290 nm.

An alternative one-electron mechanism is observed in all known heme peroxidases. In peroxidases the two one-electron oxidations 2A and 3A occur at the heme edge [12] and are not required to occur sequentially on the same substrate. Depending on the conditions the radical XA–O can escape from the peroxidase after step 2A and a polymerization reaction can occur [61].

$$X(A–O)^{\bullet}_n + XA–OH \rightarrow X(A–O)_n–A{=}O^{\bullet} + HX \qquad (k_P)$$

This competing pathway produces an insoluble polymeric product, which is not directly observed in a UV-vis assay except possibly by observing an increase in light scattering in the kinetics.

The pH in the coelom under native conditions is pH ~7.4. Under these conditions Fig. 6 shows that TBP is largely deprotonated. In other words the substrate is a phenolate above its pK_a of 6.8. Thus, an alternative mechanism (mechanism B) is:

$$1B.\ DHP + H_2O_2 \rightarrow \text{Compound I} + H_2O \qquad (k_{1B})$$

$$2B.\ \text{Compound I} + XA–O^- \rightarrow \text{Compound II} + XA–O^{\bullet} \qquad (k_{2B})$$

$$3B.\ \text{Compound II} + XA–O^{\bullet} + H^+ \rightarrow DHP + O{=}A{=}O + HX \qquad (k_{3B})$$

The difference is subtle. There is one less proton transfer step required from the active site. The difference of a diffusion step can be a significant difference for enzyme function. For example, the rate at which water diffuses out of the distal pocket is thought to account for the difference between peroxidase and catalase activity [62]. However, there is a more important difference in DHP.

The hypothesis that DHP binds the substrate as a phenolate in an internal binding site must be considered in relation to the X-ray crystal structure and other available data. A molecular model of iron-bound H_2O_2 in the 1EWA X-ray structure shown in Fig. 1 indicates that that H_2O_2 is in van der Waal's contact with the substrate analog, 4-iodophenol [4,39]. Fig. 1 shows that the phenol oxygen is at a distance of 7.7 Å from the heme iron and the ring carbons are less than 5 Å from the heme iron. If the substrate binds as phenolate, charge compensation is possible due to the presence of H55 in the vicinity of the phenolate oxygen. Histidine can be present as imidazole or imidazolium. When histidine is in the imidazolium form it can compensate the negative charge of the phenolate. The pK_a of histidine in solution is 6.9, which is comparable to that of TBP. The X-ray crystal structure does not determine the charge state of the histidine or substrate.

To date substrate binding has been studied by FTIR [54], NMR [63], and EPR [64]. One caveat is that the low solubility of TBP prevents the study of substrate binding by these methods, since they all require millimolar concentrations of protein. For this reason we have relied on two substrate analogs, 2,4,6-trifluorophenol for FTIR and EPR and 2,4,-dichlorophenol for NMR. FTIR spectroscopy provides evidence that the substrate-bound form of DHP is not observed at room temperature when CO is bound to the heme in the ferrous form of DHP [54]. We have observed that the substrate has a large effect on the CO frequencies of DHP-CO at cryogenic temperature at pH 5, but has a smaller effect at pH 7.5 or 10 [54]. One possible explanation is that substrate binding is greater at pH 5 than at the higher pH values consistent with changes in the protein interactions with bound CO [43,44,65,66]. The inhibition of substrate binding could arise from steric interactions with CO bound to the heme in a geometry nearly perpendicular to the heme plane [67,68]. ^{1}H-hyperfine NMR experiments on the metcyano form of DHP (DHP-CN) show that the CζH of Phe35 is significantly broadened in the pH 5.5 and pH 7.0 spectra [63]. The data are consistent with displacement of more than 0.5 Å when substrate binds as observed in the X-ray crystal structure. However, at pH 8.4 and pH 9.9 there is less broadening. There is a significant shift in the heme propionate at pH 7.0 and pH 8.4. The latter observation may be indicative of a second mode of binding, but this is not proven since the X-ray structure also shows displacements precisely in the propionate when the substrate 4-iodophenol binds in the internal binding pocket [4,39]. EPR spectra measured at 4 K show that the ferric form of DHP is most like metaquo (DHP-H_2O) and that this predominately low spin form becomes almost completely high spin when substrate binds at pH 6.0 [64]. The EPR spectrum at pH 10.0 is consistent with a ferric hydroxide adduct (DHP-OH) and even at this pH there is a nearly complete change in spin state when substrate binds. These data are consistent with substrate binding in an internal binding site at a range of pH values that spans its pK_a. For this reason we favor the hypothesis that the differences in mechanism apparent at various pH values are not due to a change in the binding site of the substrate.

The large difference in the observed spectral changes in the Soret band of DHP as a function of pH (Fig. 5) suggests that there is a different mechanism above and below the pK_a of TBP.

Scheme 1.

Above pH 6.8 the Soret band shifts immediately from 408 nm to 419 nm and then from 419 nm to 410 nm on a time scale that is commensurate with product formation. Although 410 nm is not far from the position of the oxy Soret band in DHP at 414 nm, the spectral features of the intermediate do not resemble the oxy form. Below pH 6.8 there is no evidence for a shift in the Soret band. The only observed spectral change observed in Fig. 5 is a decrease in intensity consistent with attack of the heme by H_2O_2 or a radical intermediate.

Since these changes are observed even in the absence of the substrate as shown in Figs. 7 and 8 there are different mechanisms of H_2O_2 activation inherent in DHP as a function of pH. We can estimate the pK_a for the open→closed transition of the distal histidine based on the fact that the crystallization buffer has pH=6.5 and both conformations of the distal histidine were observed in the crystal structure. At low pH the distal histidine is protonated and is in the open or solvent exposed conformation. Hence, the distal histidine is not available in the distal pocket to activate H_2O_2 when it binds to the heme iron. H_2O_2 activation is slowed and could proceed using the pyrrole nitrogens as an acid–base catalyst. This may increase the chance that side reactions occur such as oxidation of the heme itself as seen in Fig. 7. Above pH 6.5 the distal histidine is in the distal pocket and can act as the acid–base catalyst to activate bound H_2O_2, which resembles the activation mechanism in peroxidases [20,62].

5. Conclusion

The dichotomy of mechanisms A (phenol) and B (phenolate) discussed above has not been considered previously in peroxidase studies. Many secretory peroxidases act at pH<5.5 in the soil on substrates that are in the phenol form. In fact, the best-studied secretory peroxidase, HRP, does not oxidize substrates in the phenolate form [18,69]. In studies of DHP, we and others began by using pH ~5 conditions used in many plant peroxidase studies [1,2] following the literature on oxidation of halogenated phenols. However, the data presented here are consistent with maximum enzyme activity in the pH range from 7.0 to 7.5, which is the pH of the coelom of *A. ornata* consistent with the biological location of DHP [1,2,5,70].

The character, rate and extent of the dehalogenation reaction all change dramatically at the pK_a of the substrate ($TBP \rightarrow TBPO^- + H^+$, p$K_a$=6.8). When the pH is in the normal range for biological function (7.0–7.5) the spectral features are those of the anion $TBPO^-$ being converted to DBQ product as shown in Scheme 1.

At pH<7.0 the more rapid kinetics are also associated with a more rapid degradation of the heme due to irreversible oxidation reactions catalyzed by H_2O_2.

At the pH of the coelom, the mechanism of DHP has unique features that distinguish it from other known peroxidases. DHP can activate H_2O_2 without the amino acid residues regarded as essential in for peroxidases. DHP has an internal binding site that can bind the substrate in the phenolate form. DHP carries out two-electron transfers preferentially since the substrate is unable to diffuse away after the first oxidation step. DHP is unique among the globins as well. The internal binding pocket for substrate is an unprecedented feature in hemoglobins. The likely origin of DHP as a duplicated gene that underwent divergent evolution [47] can explain the origin of these new features given the selective pressure of brominated phenols and other natural toxic compounds in the saline mud flats where *A. ornata* is found. The findings here lead to the conclusion that DHP adapted not only to preferentially perform two-electron oxidations, but also to accommodate substrates in the phenolate form, both novel features in enzymatic catalysis by peroxidases.

Acknowledgements

We thank Prof. Clay Clark and Dr. Ruby Chen for assistance with stopped-flow experiments. SF acknowledges support through NSF MCB-9874895.

Appendix A. Supplementary data

Supplementary data associated with this article can be found, in the online version, at doi:10.1016/j.bbapap.2006.09.019.

References

[1] J. Belyea, L.B. Gilvey, M.F. Davis, M. Godek, T.L. Sit, S.A. Lommel, S. Franzen, Enzyme function of the globin dehaloperoxidase from *Amphitrite ornata* is activated by substrate binding, Biochemistry 44 (2005) 15637–15644.

[2] Y.P. Chen, S.A. Woodin, D.E. Lincoln, C.R. Lovell, An unusual dehalogenating peroxidase from the marine terebellid polychaete *Amphitrite ornata*, J. Biol. Chem. 271 (1996).

[3] Y.P. Chen, D.E. Lincoln, S.A. Woodin, C.R. Lovell, Purification and properties of a unique flavin-containing chloroperoxidase from the capitellid polychaete *Nontmastus lobatus*, J. Biol. Chem. 266 (1991) 23909–23915.

[4] M.W. LaCount, E.L. Zhang, Y.P. Chen, K.P. Han, M.M. Whitton, D.E. Lincoln, S.A. Woodin, L. Lebioda, The crystal structure and amino acid sequence of dehaloperoxidase from *Amphitrite ornata* indicate common ancestry with globins, J. Biol. Chem. 275 (2000) 18712–18716.

[5] S. Franzen, M.P. Roach, Y.P. Chen, R.B. Dyer, W.H. Woodruff, J.H. Dawson, The unusual reactivities of *Amphitrite ornata* dehaloperoxidase

and *Notomastus lobatus* chloroperoxidase do not arise from a histidine imidazolate proximal heme iron ligand, J. Am. Chem. Soc. 120 (1998) 4658–4661.
[6] R.P. Ferrari, E. Laurenti, F. Trotta, Oxidative 4-dechlorination of 2,4,6-trichlorophenol catalyzed by horseradish peroxidase, J. Biol. Inorg. Chem. 4 (1999) 232–237.
[7] A. Courteix, A. Bergel, Horseradish peroxidase-catalyzed hydroxylation of phenol. 1. Thermodynamic analysis, Enzyme Microb. Technol. 17 (1995) 1087–1093.
[8] P.J. Harvey, R. Floris, T. Lundell, J.M. Palmer, H.E. Schoemaker, R. Wever, Catalytic mechanisms and regulation of lignin peroxidase, Biochem. Soc. Trans. 20 (1992) 345–349.
[9] E. Monzani, A.L. Gatti, A. Profumo, L. Casella, M. Gullotti, Oxidation of phenolic compounds by lactoperoxidase. Evidence for the presence of a low-potential compound II during catalytic turnover, Biochemistry 36 (1997) 1918–1926.
[10] A. Bassi, Z. Geng, M. Gijzen, Enzymatic removal of phenol and chlorophenols using soybean seed hulls, Eng. Life Sci. 4 (2004) 125–130.
[11] Z.H. Geng, A.S. Bassi, M. Gijzen, Enzymatic treatment of soils contaminated with phenol and chlorophenols using soybean seed hulls, Water Air Soil Pollut. 154 (2004) 151–166.
[12] M.A. Ator, O.d. Montellano, Protein control of prosthetic heme reactivity. Reaction of substrates with the heme edge of horseradish peroxidase, J. Biol. Chem. 262 (1987) 1542–1551.
[13] B.D. Howes, J.N. RodriguezLopez, A.T. Smith, G. Smulevich, Mutation of distal residues of horseradish peroxidase: influence on substrate binding and cavity properties, Biochemistry 36 (1997) 1532–1543.
[14] A.K. Abelskov, A.T. Smith, C.B. Rasmussen, H.B. Dunford, K.G. Welinder, pH dependence and structural interpretation of the reactions of *Coprinus cinereus* peroxidase with hydrogen peroxide, ferulic acid, and 2,2′-azinobis(3-ethylbenzthiazoline-6-sulfonic acid), Biochemistry 36 (1997) 9453–9463.
[15] L.M. Landino, B.C. Crews, J.K. Gierse, S.D. Hauser, L.J. Marnett, Mutational analysis of the role of the distal histidine and glutamine residues of prostaglandin-endoperoxide synthase-2 in peroxidase catalysis, hydroperoxide reduction, and cyclooxygenase activation, J. Biol. Chem. 272 (1997) 21565–21574.
[16] D.K. Bhattacharyya, U. Bandyopadhyay, R.K. Banerjee, Chemical and kinetic evidence for an essential histidine residue in the electron-transfer from aromatic donor to horseradish-peroxidase compound-I, J. Biol. Chem. 268 (1993) 22292–22298.
[17] M.C. Foshay, L.B. Vitello, J.E. Erman, PH dependence of heme iron coordination, hydrogen peroxide reactivity, and cyanide binding in cytochrome *c* peroxidase(H52K), Biochemistry 43 (2004) 5065–5072.
[18] P.K. Patel, M.S. Mondal, S. Modi, D.V. Behere, Kinetic studies on the oxidation of phenols by the horseradish peroxidase compound II, Biochim. Biophys. Acta, Prot. Struct. Mol. Enzymol. 1339 (1997) 79–87.
[19] P.G. Furtmuller, U. Burner, G. Regelsberger, C. Obinger, Spectral and kinetic studies on the formation of eosinophil peroxidase compound I and its reaction with halides and thiocyanate, Biochemistry 39 (2000) 15578–15584.
[20] H.B. Dunford, Heme Peroxidases, Wiley-VCH, New York, 1999.
[21] D.K. Jones, D.A. Dalton, F.I. Rosell, E.L. Raven, Class I heme peroxidases: characterization of soybean ascorbate peroxidase, Arch. Biochem. Biophys. 360 (1998) 173–178.
[22] M. Zamocky, S. Janecek, F. Koller, Common phylogeny of catalase—peroxidases and ascorbate peroxidases, Gene 256 (2000) 169–182.
[23] J. Mano, C. Ohno, Y. Domae, K. Asada, Chloroplast ascorbate peroxidase is the primary target of methyl viologen-induced stress in spinach leaves: its relevance to monohydroascorbate radical detected with in vivo ESR, Biochim. Biophys. Acta 1504 (2001) 275–287.
[24] A.N.P. Hiner, J.H. Ruiz, J.N.R. Lopez, F.G. Canovas, N.C. Brisset, A.T. Smith, M.B. Arnao, M. Acosta, Reactions of the class II peroxidases, lignin peroxidase and *Arthromyces ramosus* peroxidase, with hydrogen peroxide—catalase-like activity, compound III formation, and enzyme inactivation, J. Biol. Chem. 277 (2002) 26879–26885.
[25] M. Kvaratskhelia, C. Winkel, M.T. Naldrett, R.N.F. Thorneley, A novel high activity cationic ascorbate peroxidase from tea (*Camellia sinensis*)—a class III peroxidase with unusual substrate specificity, J. Plant Phys. 154 (1999) 273–282.
[26] P.J. Wright, A.M. English, Buffer-anion-dependent Ca2+ leaching from horseradish peroxidase at low pH, J. Biol. Inorg. Chem. 6 (2001) 348–358.
[27] M. Gajhede, D.J. Schuller, A. Henriksen, A.T. Smith, T.L. Poulos, Crystal structure of horseradish peroxidase C at 2.15 angstrom resolution, Nat. Struct. Biol. 4 (1997) 1032–1038.
[28] G. Battistuzzi, M. D'Onofrio, L. Loschi, M. Sola, Isolation and characterization of two peroxidases from *Cucumis sativus*, Arch. Biochem. Biophys. 388 (2001) 100–112.
[29] U. Burner, P.G. Furtmuller, A.J. Kettle, W.H. Koppenol, C. Obinger, Mechanism of reaction of myeloperoxidase with nitrite, J. Biol. Chem. 275 (2000) 20597–20601.
[30] H.B. Dunford, R.A. Alberty, Kinetics of fluoride binding by ferric horse radish peroxidase, Biochemistry 6 (1967) 447.
[31] J. Ricard, R.J. Williams, G. Mazza, Oxidation–reduction potentials and ionization states of 2 turnip peroxidases, Eur. J. Biochem. 28 (1972) 566.
[32] T.L. Poulos, J. Kraut, The stereochemistry of peroxidase catalysis, J. Biol. Chem. 255 (1980) 8199–8205.
[33] A. Henriksen, A.T. Smith, M. Gajhede, The structures of the horseradish peroxidase C-ferulic acid complex and the ternary complex with cyanide suggest how peroxidases oxidize small phenolic substrates, J. Biol. Chem. 274 (1999) 35005–35011.
[34] M. Tanaka, K. Ishimori, M. Mukai, T. Kitagawa, I. Morishima, Catalytic activities and structural properties of horseradish peroxidase distal His42→Glu or Gln mutant, Biochemistry 36 (1997) 9889–9898.
[35] L. Bateman, C. Leger, D.B. Goodin, F.A. Armstrong, A distal histidine mutant (H52Q) of yeast cytochrome *c* peroxidase catalyzes the oxidation of H2O2 instead of its reduction, J. Am. Chem. Soc. 123 (2001) 9260–9263.
[36] L.B. Vitello, J.E. Erman, M.A. Miller, J. Wang, J. Kraut, Effect of Arginine-48 replacement on the reaction between cytochrome-c peroxidase and hydrogen-peroxide, Biochemistry 32 (1993) 9807–9818.
[37] J.N. RodriguezLopez, A.T. Smith, R.N.F. Thorneley, Role of Arginine 38 in horseradish peroxidase a critical, residue for substrate binding and catalysis, J. Biol. Chem. 271 (1996) 4023–4030.
[38] A.N.P. Hiner, E.L. Raven, R.N.F. Thorneley, F. Garcia-Canovas, J.N. Rodriguez-Lopez, Mechanisms of compound I formation in heme peroxidases, J. Inorg. Biochem. 91 (2002) 27–34.
[39] L. Lebioda, M.W. LaCount, E. Zhang, Y.P. Chen, K. Han, M.M. WHitton, D.E. Lincoln, S.A. Woodin, An enzymatic globin from a marine worm, Nature 401 (1999) 445.
[40] S. Franzen, J.L. Belyea, L.B.G. Gilvey, M.F. Davis, C. Chaudhary, T.L. Sit, S.A. Lommel, Proximal cavity, distal histidine and substrate hydrogen-bonding mutations modulate the activity of *Amphitrite ornata* dehaloperoxidase, Biochemistry 45 (2006) 9085–9094.
[41] F. Yang, G.N. Phillips Jr., Crystal structures of CO-, deoxy- and met-myoglobins at various pH values, J. Mol. Biol. 256 (1996) 762–774.
[42] T. Suzuki, Y. Watanabe, M. Nagasawa, A. Matsuoka, K. Shikama, Dual nature of the distal histidine residue in the autoxidation reaction of myoglobin and hemoglobin—comparison of the H64 mutants, Eur. J. Biochem. 267 (2000) 6166–6174.
[43] S. Franzen, An electrostatic model for the frequency shifts in the carbonmonoxy stretching band of myoglobin: correlation of hydrogen bonding and the Stark tuning rate, J. Am. Chem. Soc. 124 (2002) 13271–13281.
[44] K. Nienhaus, J.S. Olson, S. Franzen, G.U. Nienhaus, The origin of stark splitting in the initial photoproduct state of MbCO, J. Am. Chem. Soc. 127 (2005) 40–41.
[45] S. Franzen, Effect of a charge relay on the vibrational frequencies of carbonmonoxy iron porphine adducts: the coupling of changes in axial ligand bond strength and porphine core size, J. Am. Chem. Soc. 123 (2001) 12578–12589.
[46] S.F. Altschul, T.L. Madden, A.A. Schäffer, J. Zhang, Z. Zhang, W. Miller, D.J. Lipman, Gapped BLAST and PSI-BLAST: a new generation of protein database search program, Nucleic Acids Res. 25 (1997) 3389–3402.
[47] K.P. Han, S.A. Woodin, D.E. Lincoln, K.T. Fielman, B. Ely, *Amphitrite*

ornata, a marine worm, contains two dehaloperoxidase genes, Mar. Biotechnol. 3 (2001) 287–292.
[48] E. Conti, C. Moser, M. Rizzi, A. Mattevi, C. Lionetti, A. Coda, P. Ascenzi, M. Brunori, M. Bolognesi, X-ray crystal-structure of ferric aplysia-limacina myoglobin in different liganded states, J. Mol. Biol. 233 (1993) 498–508.
[49] T. Suzuki, T. Takagi, K. Shikama, Amino-acid-sequence of myoglobin from Aplysia-Kurodai, Biochim. Biophys. Acta 669 (1981) 79–83.
[50] Z.Z. Chen, J. Martin, B.T.O. Lee, Hemoglobins of Kiefferulus, sister genus of Chironomus (Diptera: Insecta): evolution of the Hb VIIB cluster, J. Mol. Evol. 41 (1995) 909–919.
[51] T. Burmester, B. Ebner, B. Weich, T. Hankeln, Cytoglobin: a novel globin type ubiquitously expressed in vertebrate tissues, Mol. Biol. Evol. 19 (2002) 416–421.
[52] D. de Sanctis, S. Dewilde, A. Pesce, L. Moens, P. Ascenzi, T. Hankeln, T. Burmester, M. Bolognesi, Mapping protein matrix cavities in human cytoglobin through Xe atom binding, Biochem. Biophys. Res. Commun. 316 (2004) 1217–1221.
[53] R.L. Osborne, L.O. Taylor, K.P. Han, B. Ely, J.H. Dawson, *Amphitrite ornata* dehaloperoxidase: enhanced activity for the catalytically active globin using MCPBA, Biochem. Biophys. Res. Commun. 324 (2004) 1194–1198.
[54] K. Nienhaus, P.C. Deng, J. Belyea, S. Franzen, G.U. Nienhaus, Spectroscopic study of substrate binding to the carbonmonoxy form of dehaloperoxidase from *Amphitrite ornata*, J. Phys. Chem. B 110 (2006) 13264–13276.
[55] J. Belyea, C.M. Belyea, S. Lappi, S. Franzen, Resonance Raman Study of Ferric Heme Adducts of Dehaloperoxidase from *Amphitrite ornata*, Biochemistry 45 (2006) 14275–14284.
[56] R.E. Weber, C.P. Magnum, H. Steinman, C. Bonaventura, B. Sullivan, J. Bonaventura, Hemoglobins of two terebellid polychaetes: *Enoplobranchus sanuigneus* and *Amphitire ornata*, Comp. Biochem. Physiol. 56A (1977) 179–187.
[57] E. Chiancone, G. Ferruzzi, C. Bonaventura, J. Bonaventura, Amphitrite-Ornata Erythrocruorin. 2. Molecular controls of function, Biochim. Biophys. Acta 670 (1981) 84–92.
[58] W.E. Royer Jr., A. Pardanani, Q.H. Gibson, E.S. Peterson, J.M. Friedman, Ordered water molecules as key allosteric mediators in a cooperative dimeric hemoglobin, Proc. Natl. Acad. Sci. U. S. A. 93 (1996) 14526–14531.
[59] H.A. Heaslet, W.E. Royer, Crystalline ligand transitions in Lamprey hemoglobin — structural evidence for the regulation of oxygen affinity, J. Biol. Chem. 276 (2001) 26230–26236.
[60] H.B. Dunford, One-electron oxidations by peroxidases, Xenobiotica 25 (1995) 725–733.
[61] M.L. Ferreira, UV/visible study of the reaction of oxidoreductases and model compounds with H2O2, Macromol. Biosci. 3 (2003) 179–188.
[62] H.B. Dunford, How do enzymes work? Effect of electron circuits on transition state acid dissociation constants, J. Biol. Inorg. Chem. 6 (2001) 819–822.
[63] M.F. Davis, H. Gracz, J. Belyea, L.B. Gilvey, S.M. Decatur and S. Franzen, Binding of Both the Phenol and Phenolate Forms of the Substrate in the Hemoglobin Dehaloperoxidase from *Amphitrite ornata*, J. Am. Chem. Soc. (submitted for publication).
[64] J. Belyea, R. MacArthur, T. Smirnova and S. Franzen, Substrate Binding Triggers a Change in the Iron Spin State in Dehaloperoxidase from *Amphitrite ornata*, Proc. Natl. Acad. Sci. U.S.A. (in preparation).
[65] J. Phillips, M.L. Teodoro, T. Li, B. Smith, J.S. Olson, Bound CO is a molecular probe of the electrostatic potential in the distal pocket of myoglobin, J. Phys. Chem. B 103 (1999) 8817–8829.
[66] S. Franzen, Carbonmonoxy rebinding kinetics in H93G myoglobin: separation of proximal and distal side effects, J. Phys. Chem. B 106 (2002) 4533–4542.
[67] D. Ivanov, J.T. Sage, M. Keim, J.R. Powell, S.A. Asher, P.M. Champion, Determination of CO orientation by single-crystal infrared linear dichroism, J. Am. Chem. Soc. 116 (1994) 4139–4140.
[68] J. Vojtechovsky, K. Chu, J. Berendzen, R.M. Sweet, I. Schlichting, Crystal structures of myoglobin–ligand complexes at near-atomic resolution, Biophys. J. 77 (1999) 2153–2174.
[69] J.E. Critchlow, H.B. Dunford, Studies on horseradish-peroxidase. 9. Kinetics of oxidation of para cresol by compound II, J. Biol. Chem. 247 (1972) 3703.
[70] M.P. Roach, Y.P. Chen, S.A. Woodin, D.E. Lincoln, J.H. Dawson, Notomastus lobatus chloroperoxidase and *Amphitrite ornata* dehaloperoxidase both contain histidine as their proximal heme iron ligand, Biochemistry 36 (1997) 2197–2202.